

# GEOCHEMISTRY AND SHALE GAS POTENTIAL OF THE GARBUTT FORMATION, LIARD BASIN, BRITISH COLUMBIA (PARTS NTS 094N, O; 095B, C)

Filippo Ferri<sup>1</sup>, Adrian S. Hickin<sup>1</sup> and David H. Huntley<sup>2</sup>

---

## ABSTRACT

*An examination of the Garbutt Formation was undertaken in the Liard Basin of British Columbia to better understand the geochemical composition of the unit and how it relates to overall lithostratigraphy and shale gas potential. The Garbutt Formation is approximately 285 m thick in the Toreva–Scatter River area and consists of dark grey to black or dark grey brown shale, siltstone and lesser fine sandstone. Sedimentary structures suggest deposition by turbiditic flows below the storm wave base, which is consistent with a position near the shelf edge or prodelta environment. Rock-Eval data show average total organic carbon contents of 1.12 wt.% with peaks between 1.2 and 1.67%. The kerogen is type III in nature and average hydrocarbon abundances in kerogen are 60 mg HC/g TOC. The  $T_{max}$  maturation levels suggest the beginning of the dry gas generation window. The concentration of Mn, Fe, V and other elements suggest the sediments were deposited near the boundary between anoxic and oxic water conditions.*

Ferri, F., Hickin, A. S. and Huntley, D. H. (2011): Geochemistry and shale gas potential of the Garbutt Formation, Liard Basin, British Columbia (parts of NTS 094N, O; 095B, C); in Geoscience Reports 2011, *BC Ministry of Energy and Mines*, pages 19–36.

<sup>1</sup>Geoscience and Natural Gas Development Branch, Oil and Gas Division, BC Ministry of Energy and Mines, Victoria, BC; Fil.Ferri@gov.bc.ca

<sup>2</sup>Geological Survey of Canada, Natural Resources Canada, Vancouver, BC

**Key Words:** northeast BC, Liard River, Liard Basin, Fort St. John Group, Garbutt Formation, Scatter Formation, Rock-Eval, litho-geochemistry, gamma ray, shale gas, correlations

---

## INTRODUCTION

British Columbia has an abundance of shale intervals with unconventional gas potential and their recent exploration has increased British Columbia's natural gas resources by several trillion cubic feet (Adams, 2009). Although Triassic and Middle Devonian shale sequences have been the focus of exploration and development (e.g., Groundbirch area and Horn River Basin), other organic-rich shale and siltstone successions, such as rocks of Jurassic and Cretaceous ages, may hold potential for shale gas.

This report details the results of an examination of an Early Cretaceous shale sequence, the Garbutt Formation, found along the western margin of the Liard Basin in the Toad River map area (NTS 094N). The main objective is a characterization of this formation through lithological description and lithological and organic geochemistry. In addition, a gamma-ray spectroscopic survey of the outcrop is used to assist with correlating the section with subsurface sequences in the Liard and Horn River basins. We hope that this information will assist in the regional evaluation of this formation for its shale gas potential.

This study is part of a collaborative program between the Geological Survey of Canada and the British Columbia

Ministry of Energy and Mines and is under the federal government's Geo-mapping for Energy and Minerals (GEM) program, which is examining petroleum-related geoscience of the Liard and Horn River basins. A large part of this program has targeted mapping of surficial geology in support of drilling and completion of shale gas wells (Huntley and Hickin, 2010; Huntley and Sidwell, 2010; Huntley and Hickin, 2011; Huntley et al., 2011).

## LOCATION

The Liard Basin is located in northeastern British Columbia and includes the region where British Columbia, the Northwest Territories and the Yukon meet (Figures 1 and 2). The Liard Basin encompasses the corners of NTS map areas 094N and O, and 095 B and C. This area defines a relatively high plateau between the southern Selwyn Mountains and northern Rocky Mountains. Highway 77 runs north-south along the eastern margin of the Liard Basin. The south end of Highway 77 joins the east-west-running Alaska Highway (Highway 97) near Fort Nelson (Figure 2). Numerous petroleum activity roads and forestry access roads extend from these two main highways across the area. Road access

across the Liard River is by barge, which originates at Fort Liard, NWT and ferries vehicles to just south of the confluence of La Biche River, where a road connects to the Beaver River gas field (Figure 3).

## REGIONAL GEOLOGY

The Liard River traverses the Liard Basin, which was originally defined on the basis of the thick Late Paleozoic succession in southeastern Yukon by Gabrielse (1967) and extended into northeastern British Columbia by Morrow et al. (1993) and Richards et al. (1994). The Bovie Lake structure marks the eastern margin of the basin, west of which is an anomalously thick section of the Mississippian Mattson Formation. Late Cretaceous movement on this fault has

also preserved a thick sequence of Early to Late Cretaceous rocks within the confines of the basin (Leckie et al., 1991; Leckie and Potocki, 1998).

In the Liard River region, Cretaceous rocks rest unconformably on Triassic strata. The basal part of this section is represented by Lower to mid-Cretaceous rocks of the Fort St. John Group followed by Upper Cretaceous strata of the Dunvegan, Kotaneelee and Wapiti formations (Figures 2–4). Fort St. John Group strata represent a marine incursion along the western interior of the continent and are dominated by shale and siltstone punctuated by coarser, regressive sandstone sequences reflecting increased tectonism to the west (Chinkeh, Scatter and Sikanni formations; Stott, 1982; Leckie et al., 1991). Coarse clastic rocks of the Dunvegan Formation rest conformably on the Fort St. John Group and represent the last major regression into the

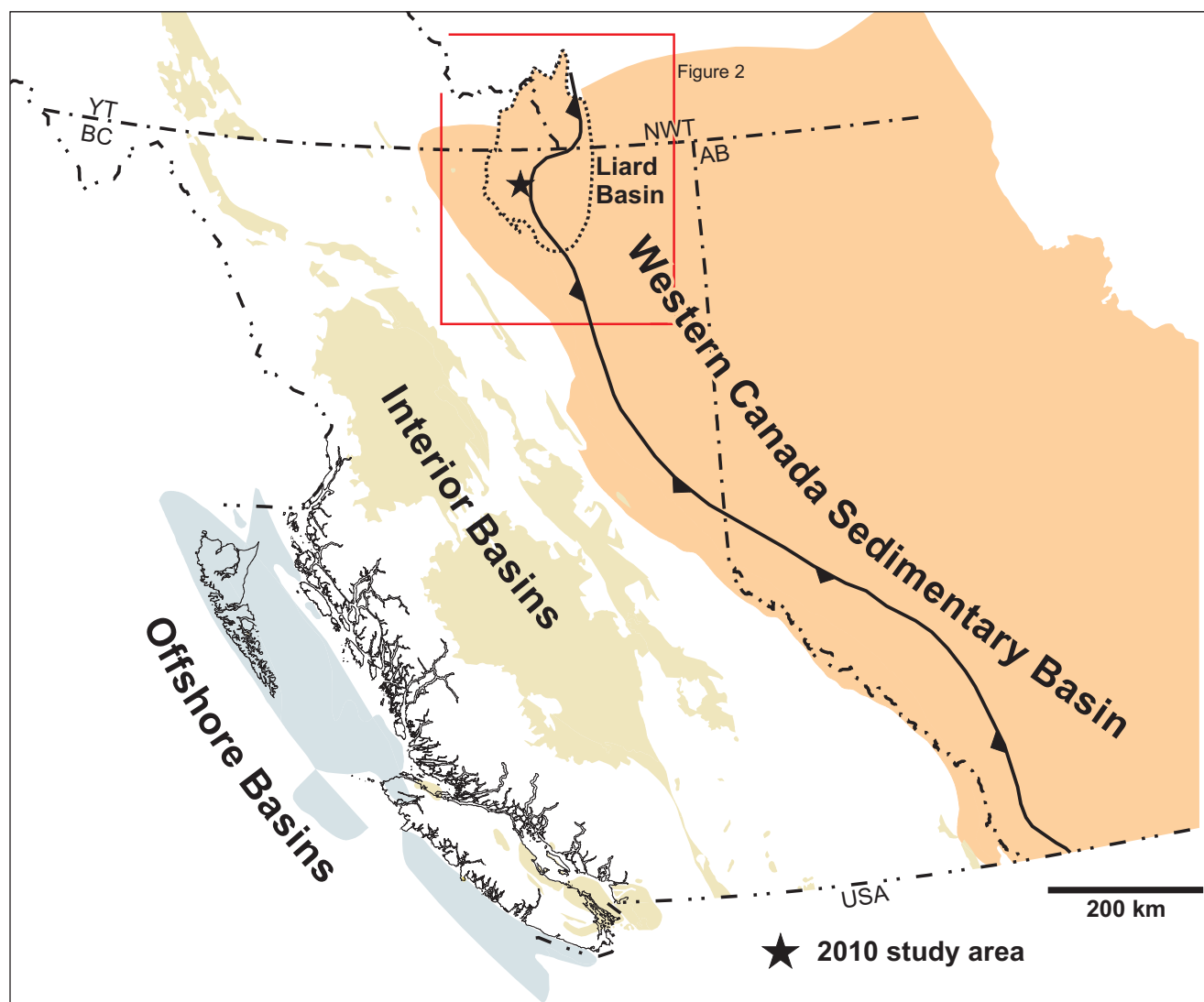


Figure 1. Location of the Liard Basin with respect to the primary sedimentary basins of Western Canada. Also shown are the Early Paleozoic offshelf depocentres of the Selwyn Basin and the Kechika Trough. The red box outlines the area shown in Figure 2. Basin outlines are from Mossop et al. (2004).

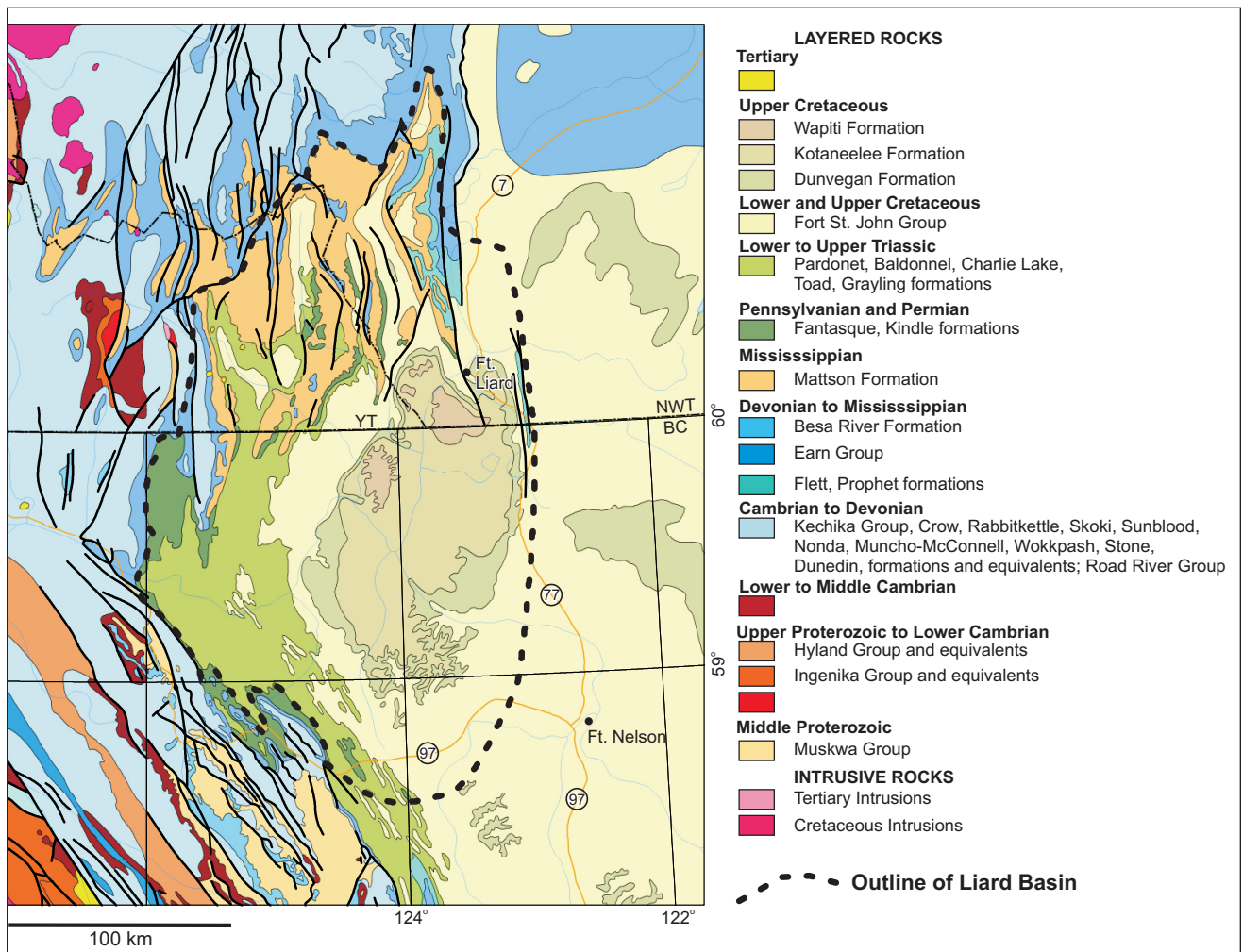


Figure 2. Geology of the Liard Basin and immediate area showing the distribution of Mattson Formation sandstone in the northern part of the Liard Basin.

interior seaway. Marine shale and minor sandstone of the Kotaneelee Formation unconformably overlie the Dunvegan Formation and define a final marine transgression that is succeeded by nonmarine sandstone and mudstone of the Wapiti Formation (Dawson et al., 1992; Taylor and Stott, 1999).

Shale, siltstone and fine sandstone of the Garbutt Formation define a major marine transgression along the Western Canada Sedimentary Basin. These rocks lie above the Chinkeh Formation, which consists of a marine shoreface succession in its upper part resting on nonmarine valley fill in its lower part (Leckie et al., 1991). Basal Garbutt Formation shale or siltstone either lie conformably atop the Chinkeh Formation (when developed) or unconformably above older strata (e.g., Triassic), with or without the presence of a pebble lag at its base (Leckie and Potocki, 1998).

Garbutt Formation rocks are interpreted to have been deposited in a marine environment, largely below the storm wave base (Leckie and Potocki, 1998). Succeeding sandstones of the Scatter Formation suggest an open-water,

shallow marine shelf to shoreface depositional setting (Leckie and Potocki, 1998). Leckie and Potocki (1998) describe wave and combined flow ripples and hummocky cross-stratification in the upper third of the Garbutt Formation, suggesting shallow-water environments affected by storm waves. Slump features within the lower parts of the Garbutt Formation, together with other mass flow deposits, suggest deposition of this unit in deeper waters, downslope from a shelf or slope-margin setting (Leckie and Potocki, 1998) or in a prodelta environment (Stott, 1982).

In British Columbia, the regional geological database in the vicinity of the section includes mapping within the Toad River (Taylor and Stott, 1999), the Tuchodi Lakes (Stott and Taylor, 1973) and the Rabbit River (Gabrielse, 1963; Ferri et al., 1999) map areas. In the Yukon and the Northwest Territories, parts of the La Biche River map area (NTS 095C) have been compiled at 1:50 000 (Fallas, 2001; Fallas and Evenchick, 2002) and 1:100 000 scales (Fallas et al., 2004). Stott (1982) first defined the type sections of the Garbutt Formation as part of a regional investigation of

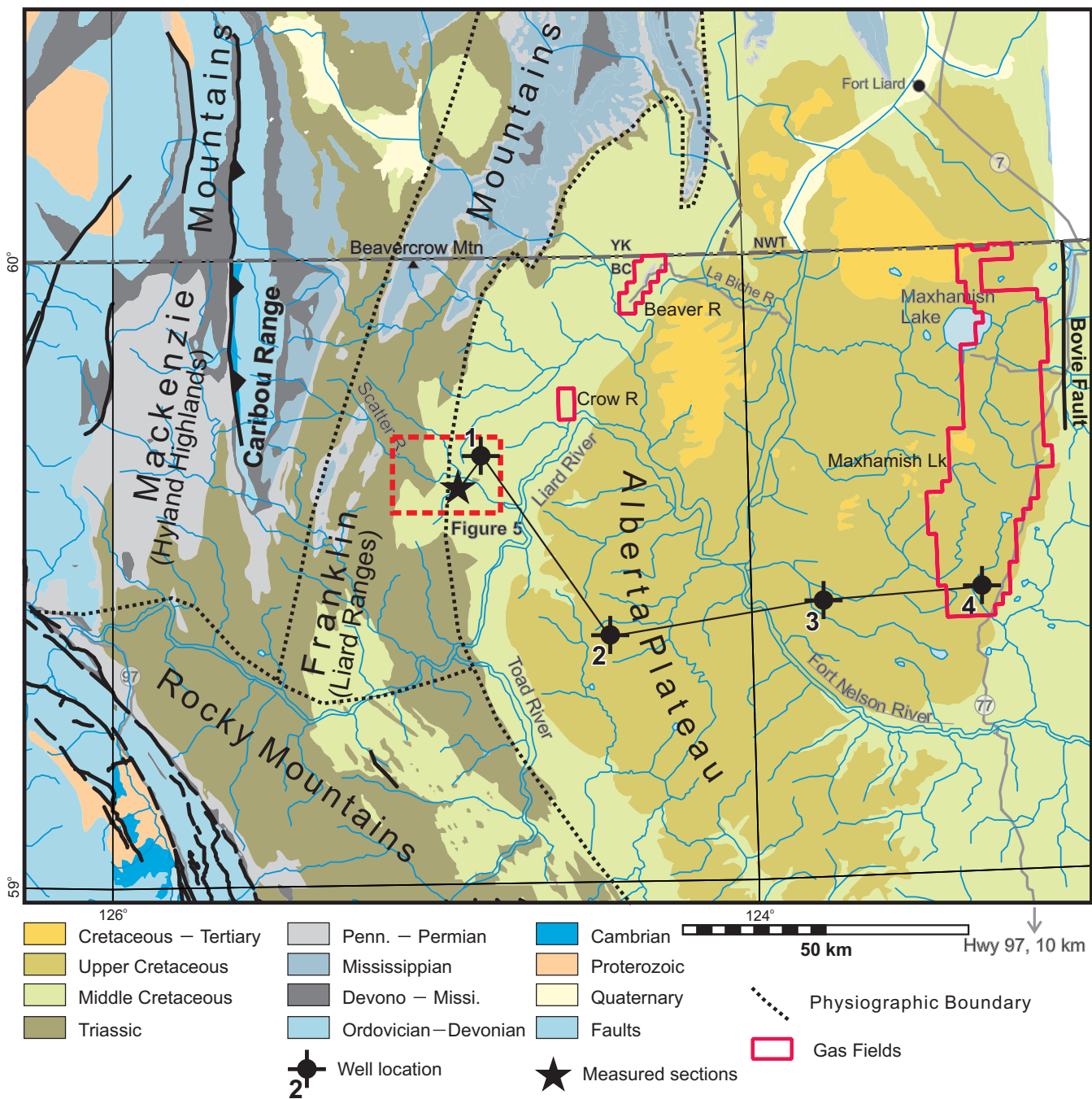


Figure 3. Regional geological setting of the study area showing main geological units and main physiographic boundaries. Wells shown in Figure 23 are marked as 1 (d-98-F), 2 (d-75-E), 3 (b-43-K) and 4 (d-52-K).

Cretaceous rocks in northeastern British Columbia. Leckie et al. (1991) and Leckie and Potocki (1998) further describe the sedimentology of the Chinkeh, Garbutt and Scatter Formations. Jowett and Schröder-Adams (2005) described the paleoenvironments and stratigraphy of the succeeding Lepine Formation. Chalmers and Bustin (2008a, b) examined the Garbutt Formation as part of more regional investigation of the shale gas potential of Lower Cretaceous shale in northeastern British Columbia.

## METHODOLOGY

Several sections of the Garbutt Formation were measured and described through the use of a 1.5 m staff along Toreva Creek and Scatter River (Figures 4 and 5). A continuous section of this unit could not be measured because of limited access and poor exposure; therefore, the five separate segments that were examined represent different, though nearly contiguous parts of the formation (Figure 5; UTM coordinates for the base of each section

	Liard River (Stott, 1982; Leckie et al., 1991)	Sikanni Chief River (Stott, 1982)	Plains, BC (Stott, 1982; Jowett and Schroder-Adams, 2005)	Plains, BC (Stott, 1982; Jowett and Schroder-Adams, 2005)	
U Cret	Dunvegan Fm	Dunvegan Fm	Dunvegan Fm	Dunvegan Fm	
Lower Cretaceous	Albian	Sully Fm	Sully Fm	Shaftesbury Fm	
	Fort St. John Group	Sikanni Fm	Sikanni Fm	Goodrich Fm	
	Lepine Fm	Buckingham Fm	Hasler Fm	Shaftesbury Fm	
	Scatter Fm		Boulder Ck Fm	Paddy Mbr	
	Tussock Mbr		Hulcross Fm	Cadotte Mbr	
	Wildhorn Mbr		Gates Fm	Harmon Mbr	
	Bulwell Member		Moosebar Fm	Notikewin Mbr	
	Garbutt Fm	Fort St. John Group	Peace River Fm	Falher Mbr	
	BIA		Chinkeh Fm	Spirit River Fm	Wilrich Mbr
			Gething Fm	Bluesky Fm	

Figure 4. Correlation of Early Cretaceous strata in northeast British Columbia.

are: 1, 394932E 6612890N; 2, 394286E 6612364N; 3, 394159E 6612554N; 4, 389260E 6612795N; 5, 389021E 6612714N; Zone 10, NAD83). Representative chip samples were acquired across 2 m intervals along the entire section. Samples were split, with one group being analyzed for whole-rock, trace and rare earth element abundances by inductively coupled plasma–emission spectroscopy (ICP-ES) and inductively coupled plasma–mass spectrometry (ICP-MS) via a lithium metaborate-tetraborate fusion at Acme Analytical Laboratories (Vancouver, BC), and a second group, at 4 m spacings, for Rock-Eval analysis at Geological Survey of Canada (GSC) laboratories (Calgary, Alberta). A smaller subset of these samples will also be analyzed by X-ray diffraction (XRD) at the GSC laboratories for semi-quantitative determination of mineral abundances. Separate samples were collected for thermal maturity determination at the GSC laboratories in Calgary through reflected light microscopy. In addition, a handheld gamma-ray spectrometer (RS-230 by Radiation Solutions Inc.) was used to measure natural gamma radiation every 1 m during a 2 minute time interval allowing the calculation of K (%), U (ppm), Th (ppm) and total gamma-ray count. These data produced a diagram showing the variation in total natural radiation along the section, which is approximately equivalent to the subsurface gamma-ray trace. This was used to assist with the correlation of the outcrop section with equivalent rocks in the subsurface.

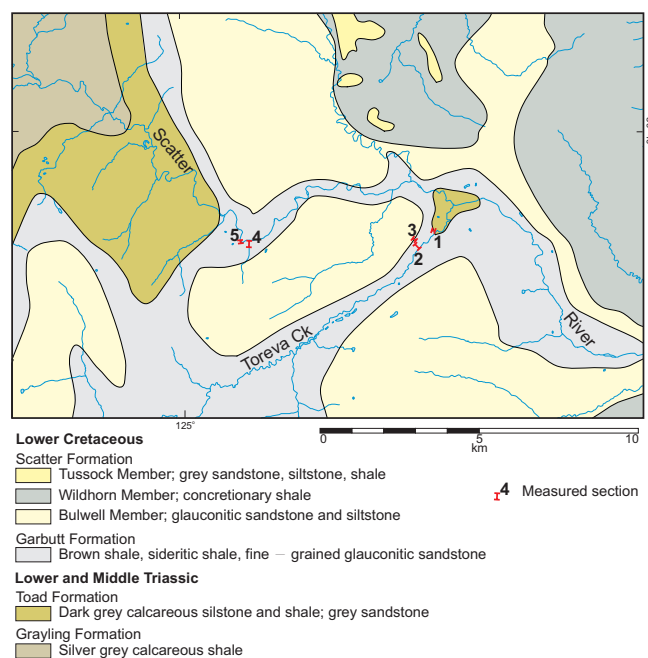


Figure 5. Location of the five measured sections of the Garbutt Formation with respect to local geology.

## LITHOLOGICAL DESCRIPTION

A combined thickness of approximately 221 m of section was measured at five localities (Figures 5–8). A composite section with the relative position of each section (Figure 6) is based on structural sections, relative position of these sections to the Toad (Triassic) and Scatter (Lower Cretaceous) formation contacts and from the 285 m section of measured Garbutt Formation (Stott, 1982) near these localities. The relative position of these sections is supported by a well-defined geothermal gradient produced by plotting  $T_{max}$  versus depth (see discussion below).

The base of the composite section was observed on Toreva Creek where more than 6 m of section is exposed. At the river level, 3 m of Toad Formation is present. It consists of thin bedded, laminated, calcareous siltstone and thin to crossbedded, fine-grained sandstone. The contact between the Toad and the Garbutt formations appears unremarkable except for the presence of 1–3 cm of grey chert nodules. The Garbutt Formation consists of dark grey crumbly shale with uneven partings and a 30 cm thick laminated bed of fine-grained, calcareous and micaceous sandstone containing carbonaceous partings in places.

The succeeding part of the Garbutt Formation was examined on the south side of Scatter River (sections 4 and 5; Figure 5), as most of the lower 60 m of the Garbutt Formation is covered in Toreva Creek (Figure 6). At Scatter River, the unit consists of rusty to dark brown weathering, micaceous shale and siltstone with thin, laminated quartz sandstone (locally glauconitic) horizons that typically comprise less than 10% of the section, but can locally reach

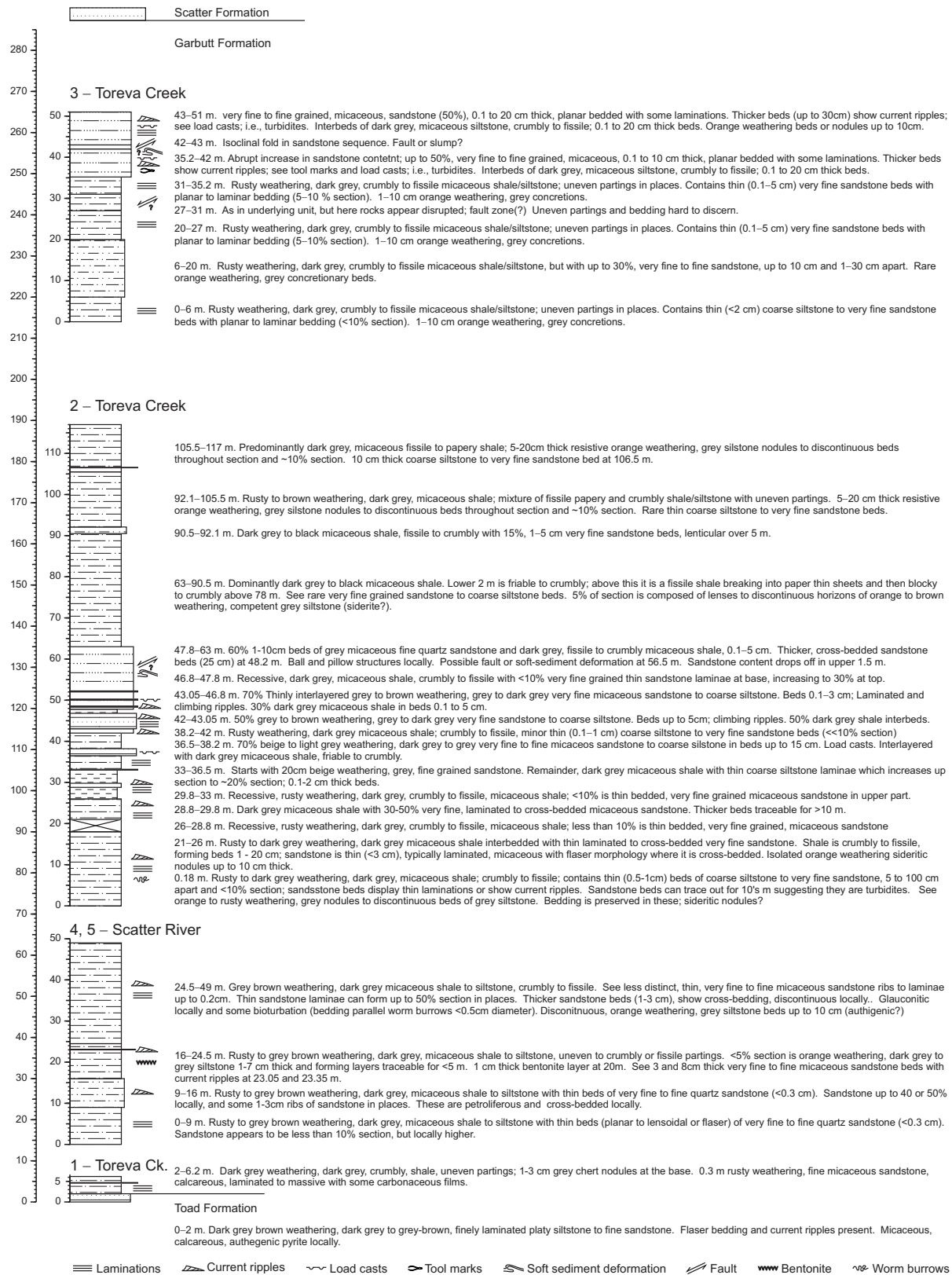


Figure 6. Relative stratigraphic positions of measured sections, with descriptive notes. Numbers refer to the order in which the sections were measured. Sections 4 and 5 are contiguous, section 4 extending from 0 to 16 m.



Figure 7. a) Looking northwest at the contact between the Garbutt and Scatter formations. Note the increase in sandstone in the upper part of the Garbutt Formation until the sandstone becomes dominant within the Scatter Formation (brown weathering sandstone); b) looking northwest at Garbutt Formation rocks measured on the north side of Toreva Creek. Note the tabular nature of the sandstone beds and how they can be traced for many tens of metres. Recessive papery shale in the upper part of section 2 and lower part of section 3 can be seen at the top of the section above the sandstone ribs. Note the structural offset of the topmost, thickest sandstone rib.



Figure 8. Looking south at the section of Garbutt Formation measured along Scatter River. Sandstone ribs seen at the top of this section are believed to be the same as those seen within the lower part of section 2 (Figure 7). Thin bentonite horizons occur at the base of the section.

up to 50%. Sandstone beds in well exposed blocks on the creek bed show lensoidal to flaser structures associated with bioturbation and may indicate wave influence (Figure 9, inset). Thicker, current-rippled sandstone beds up to 8 cm thick occur and can have a petroliferous odour when broken. Also present are discontinuous, orange-weathering manganiferous (?) siltstone horizons up to 10 cm thick, comprising 5% of the section. A thin (1–2 cm) bentonite horizon was observed at the 20 m level. Bedding-parallel trace fossils (burrows) were common in the sandy horizons (Figure 9).



Figure 9. Bedding-parallel worm burrows in lower Garbutt Formation siltstone and shale along Scatter River. Inset shows thin-bedded, planar to lenticular nature of bedding in the lower part of the Garbutt Formation, together with worm burrows (to the left of the lens cap).

Similar rock types are found in the lower part of the next stratigraphically higher section examined at creek level along Toreva Creek (section 2; Figure 6). The occurrence of thin bedded and laminated, fine micaceous sandstone begins to increase at the 33 m level of this section. Sandstone beds thicken (10–15 cm) and constitute up to 60% of the section by the 60 m level, and locally up to 70% between 43 and 48 m. Occasionally, the sandstone beds can be up to 25 cm thick and contain climbing to current ripples and load casts at the base (Figure 10). These beds form prominent sheets traceable for tens of metres (Figure 7).

There is a possible fault or soft-sediment deformation structure at the 56.5 m level of section 2 (Figure 11). Flat-lying siltstone and fine sandstone sit abruptly above folded and locally overturned siltstone and sandstone (Figure 11). The tightness of the folding and the manner in which the folded beds are cut off along strike suggests a tectonic feature.

At 63 m of section 2, the sandstone content drops off over 1.5 m, followed by 50 m of dark grey to black, fissile to papery, micaceous shale with rare, thin beds of fine micaceous sandstone (Figures 6 and 12). At the 117 m level, section 2 became obscured by vegetation; as a result, a new



Figure 10. Current ripples in fine sandstone of the Garbutt Formation within the lower part of section 2.

section was initiated approximately 1 km to the west.

The lower part of section 3 (Figure 6) contains fissile shale similar to the lower part of section 2. Lenticular to podiform, orange-weathering, manganiferous (?) siltstone horizons are found within the finer-grained sequences (Figure 13). Thin-bedded, laminated sandstone increases up-section until it comprises approximately 30% of the



Figure 11. Possible fault (or soft-sediment deformation feature?) in the Garbutt Formation at 56.5 m of section 2.

section (6–20 m). At the 35 m level, micaceous sandstone beds increase in abundance and thickness and are locally up to 30 cm thick. Sandstone beds are tabular in nature, commonly laminated and traceable for many metres along the section. Thicker beds show current ripples (Figure 14), load casts and tool marks (Figure 15). Numerous zones of disrupted bedding were observed in the section (Figures 16 and 17) being of either soft-sediment or tectonic origin. The section is too steep to access at the top of section 3, but observations indicate that sandstone abundances continue to increase upsection to the base of the Scatter Formation (i.e., at the first thick sandstone horizon, approximately 20–25 m higher in the section).



Figure 12. Black to dark grey, thin papery shale in the upper part of section 2.

## INTERPRETATION

Overall, the combined sections of the Garbutt Formation define a coarsening-upwards succession to the Scatter Formation. The minor coarsening-upwards interval in the middle of section 2 along Toreva Creek (Figure 6) likely represents a lower-order succession. Generally, the Garbutt Formation appears to represent a shallowing-upward transition from distal shelf/slope margin to inner shelf and shoreface. The lower Garbutt Formation consists of interbedded, laminated mudstone and thin tabular sandstone



Figure 13. Interbedded sandstone, shale and siltstone in the upper part of section 3.



Figure 14. Current ripples in fine sandstone of the Garbutt Formation in the upper part of section 3.



Figure 17. Soft-sediment deformation or folding in Garbutt Formation rocks in the upper part of section 3.



Figure 15. Tool marks (aligned with the pencil) along the base of sandstone beds in the upper part of section 3.



Figure 16. Soft-sediment deformation or faulting in Garbutt Formation rocks in the upper part of section 3 (indicated with the arrow).

with current and climbing ripples, load and tool casts and bedding plane-parallel trace fossils that have low diversity but are abundant. This suggests deposition by turbid flow at the slope margin or possibly distal shelf. The increase in sand content upsection reflects a more proximal position with respect to terrigenous sediment supply. In the upper portion of the Garbutt Formation, sheet sand beds become more common and thicker and may represent sea level lowering or the progradation of a Scatter Formation delta. This succession supports the interpretation that the Garbutt Formation formed initially in a slope-margin setting (Leckie and Potocki, 1998) or a distal shelf, prodelta environment (Stott, 1982). Convoluted bedding in the upper part of the Garbutt Formation (or in the middle coarsening sequence), if of depositional origin, would indicate instability. In these settings, turbidite deposits were shed from the shelf edge or delta into quiescent waters. Though storm beds were not unequivocally identified in this investigation, Leckie and Potocki (1998) report wave-formed structures in the upper part of the Garbutt Formation and conclude they formed as relative sea level became shallower prior to the deposition of the Scatter Formation.

## ROCK-EVAL DATA

Only a summary of the Rock-Eval data will be presented here; the complete dataset will be made available in a later publication. Plotting of total organic carbon (TOC) within the section indicates that the highest TOC levels (1.2–1.67%) are within the central part of the formation (Figure 18), with an average value for the entire sample set of 1.12%. Distribution of other Rock-Eval parameters suggests that the kerogen within these sedimentary rocks is type III in nature; i.e., terrestrial plant in origin (Figures 19a, b) and has an average hydrogen index (HI) of 60 mg HC<sup>1</sup> /g TOC (Figure 19b), although prior to maturation, this would have been slightly higher (Figures 18 and 19c).

Thermal maturation of the sequence can be reasonably deduced from  $T_{max}^2$  values, as  $S2^3$  values are consistently higher than 0.2 mg HC/g rock (Peters, 1986). Plotting  $T_{max}$  versus depth in the section shows a regular increase in  $T_{max}$  values with increase in depth likely related to the paleogeothermal gradient (Figure 18). A regression line through the dataset indicates that the top of the section is at the beginning of the dry gas generation window and the base is at the midpoint (Dow, 1977; Teichmuller and Durand, 1983; cf. Figure 4 in Leckie et al., 1988).

Although organic carbon levels suggests a fair to good source rock (Peters, 1986), HI levels are low due to a type III kerogen and suggest gas-prone kerogen. The presence of trace fossils in parts of the sequence, together

with litho-geochemistry (see below), suggests that optimum reducing conditions (i.e., anoxic) were not present for preservation of all organic material (i.e., some was metabolized by organic activity). This may have also been coupled with low productivity and dilution by sediment supply.

## SCINTILLOMETER DATA

Gamma-ray spectroscopic data (total counts as dose, with calculated U, Th and K concentrations) collected across the various sections of the Garbutt Formation are displayed in Figure 20. At first glance, it appears that the total count rate (i.e., gamma-ray trace) correlates best with

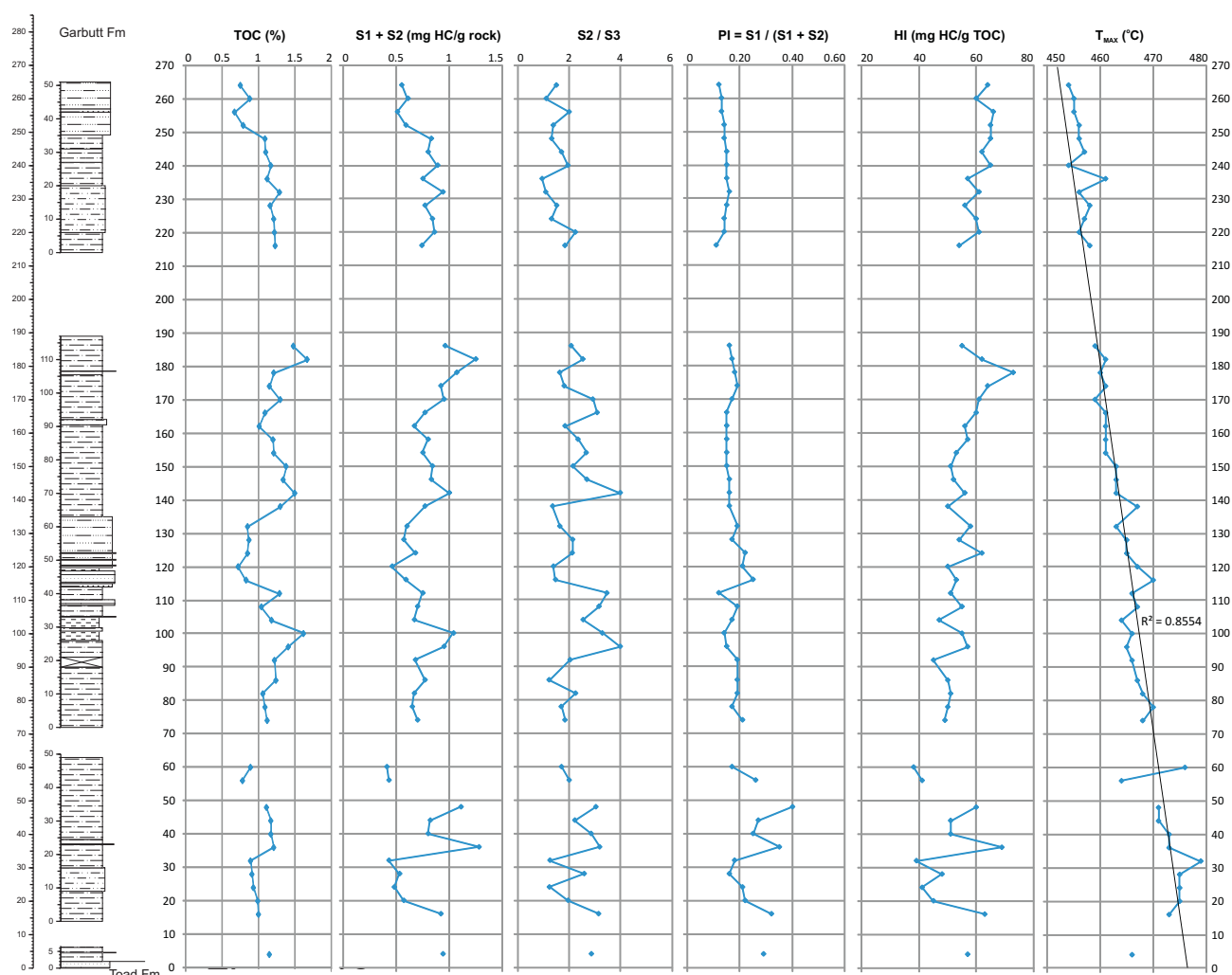


Figure 18. Rock Eval data plotted against the measured sections of the Garbutt Formation.

- 1 Hydrocarbons
- 2 Maximum temperature of hydrocarbon production
- 3 Represents the amount of hydrocarbons resulting from cracking sedimentary organic matter in the sample (mg HC/g rock)

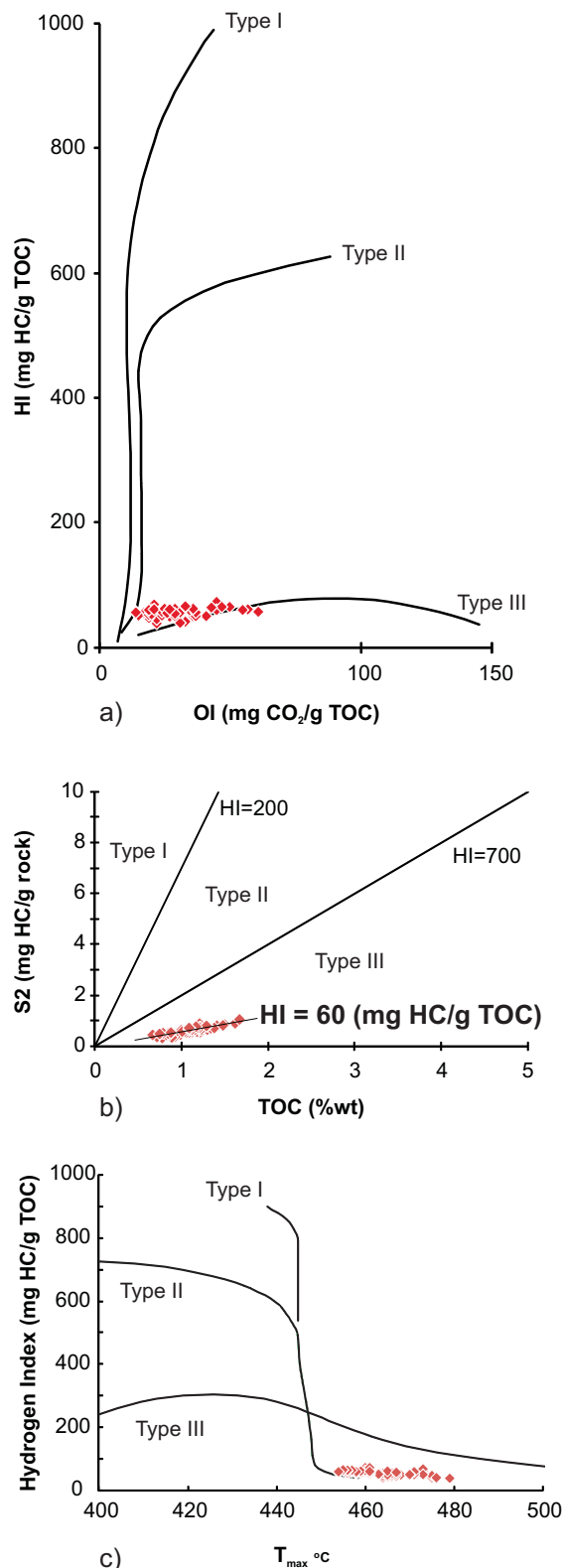


Figure 19. a) Modified van Krevelen diagram (Tissot and Welte, 1984) showing the type III nature of the kerogen from the Garbutt Formation. b) An S<sub>2</sub> versus TOC diagram from Langford and Blanc-Valleron (1990) showing the type III nature of the kerogen from the Garbutt Formation and the level of hydrocarbons in the organic matter (60 mg HC/g TOC); c) Hydrogen index (HI) versus T<sub>max</sub> showing the change in hydrocarbon content with maturation of the kerogen; modified from Bordenave (1993).

K and Th concentrations, suggesting that the overall bulk concentration of the rocks is controlling the signature. This contrasts with similar data from the Triassic Toad Formation and Devonian-Mississippian Besa River Formation, where the total gamma-ray trace is governed by the concentration of U, which is ultimately tied to reducing conditions at the time of deposition (Ferri et al., 2010, 2011). Furthermore, this reducing environment in Toad River and Besa River rock types results in the relative abundance of organic matter (shown as TOC), correlating very well with U concentrations (Ferri et al., 2010, 2011). Although there is a broad correlation between organic carbon content and total gamma-ray levels in the Garbutt Formation (Figure 20), this is likely a function of dilution within the coarser clastic parts of the succession.

## LITHOGEOCHEMICAL DATA

Select major- and trace-element geochemistry across the measured section of the Garbutt Formation is shown in Figures 21 and 22. As expected, SiO<sub>2</sub> content follows gross lithological composition and has inverse relationships with Al<sub>2</sub>O<sub>3</sub> and K<sub>2</sub>O. Concentrations of Fe<sub>2</sub>O<sub>3</sub> are above 15% by weight and average 6%. Levels of MnO and MgO mimic those of Fe<sub>2</sub>O<sub>3</sub> with levels of MnO peaking above 0.1% (averaging 0.027%) and MgO peaking above 2% (averaging 1.12%). The relative abundances of several trace elements shown in Figure 22 appear to correlate with total organic carbon contents (TOC; i.e., V, Pb and to a lesser extent Mo). Barium concentrations are quite high, up to 1500 ppm (0.15 wt.%), and these relative levels also generally follow those of TOC.

The concentration of organic carbon and specific elements within a sedimentary succession is a reflection of reducing conditions during the time of deposition (see Ferri et al., 2011 for further discussion). Quinby-Hunt and Wilde (1994) describe four groups of low-calcic shale (Table 1) based on Mn, Fe and V concentrations, which are primarily a function of the redox conditions during sediment deposition.

Chemical data for shale within the Garbutt Formation suggests they fall within Group 2 as defined by Quinby-Hunt and Wilde (1994; Table 1). These authors caution that the elemental concentrations defining Group 2 shale could form under several reducing environments such that the high Fe concentrations reflects Fe as oxides (least reduced) or sulphides (most reduced). Although the oxidation state of the Fe in the samples was not determined or any mineral speciation carried out, the low concentration of S in these rocks (average of 0.1 wt.%) suggests Fe is not found as sulphides. Furthermore, Quinby-Hunt and Wilde (1994) indicate that shale deposited in the least reducing anoxic environment will contain glauconite and other Fe silicates together with siderite and rhodochrosite and that the shale

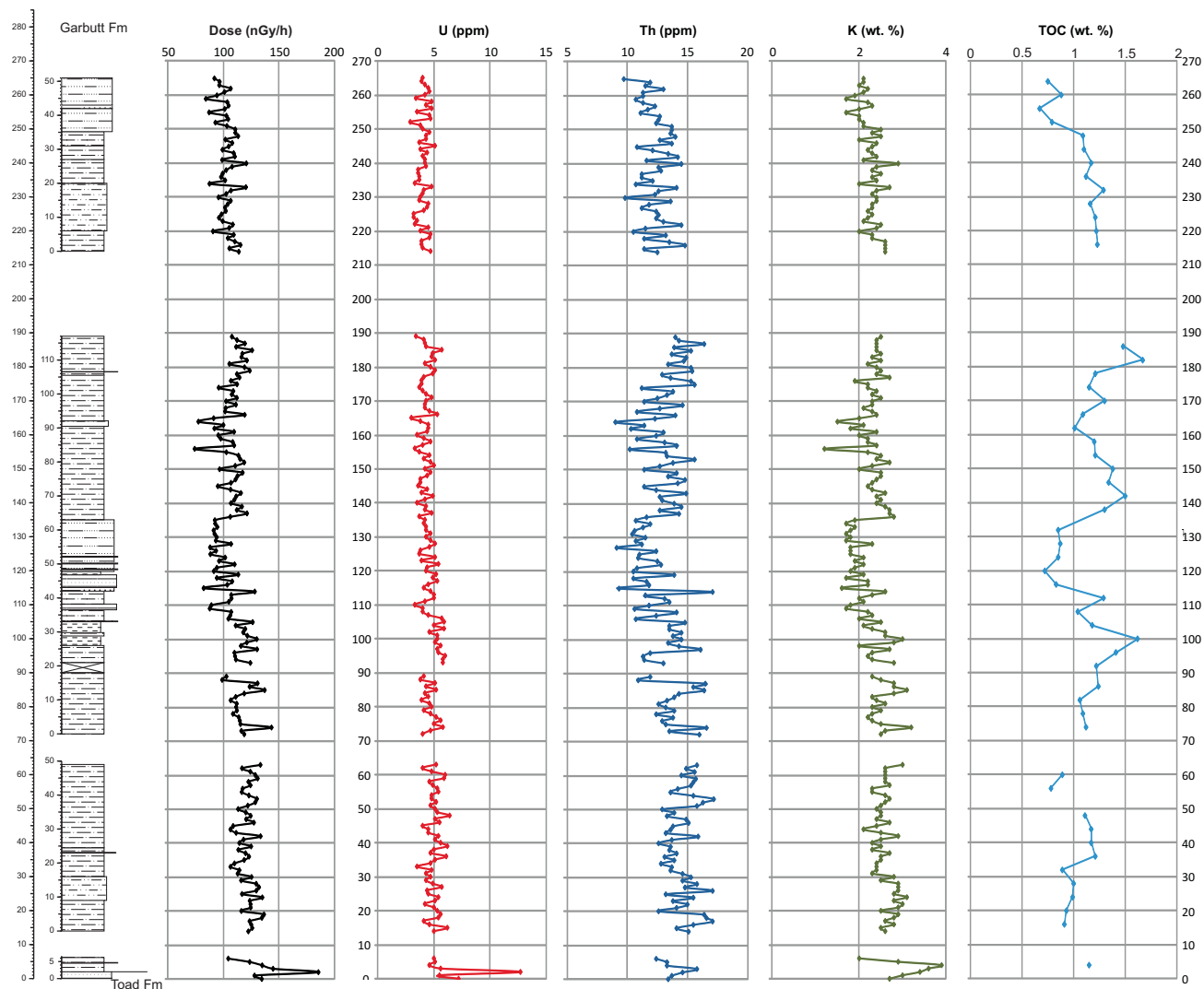


Figure 20. Gamma-ray spectrometer data and total organic carbon contents, and U, Th and K values from the five measured sections of the Garbutt Formation.

would have a browner colour due to the presence of Fe oxides.

Although the Fe concentration in sediments deposited within the oxic zone is comparable to those set down in the least anoxic conditions, the distinguishing feature is the greater abundance of Mn (Table 1), which would be found as oxides (Quinby-Hunt and Wilde, 1994). Manganese levels in Garbutt rocks average approximately 0.03%, suggesting that the bulk of the section is consistent with Group 2 anoxic rocks, but several horizons peak above 0.1% and fall within the oxic zone (Figure 21, Table 1). Also note that parts of the section have MnO levels below 0.01% (suggesting more reduced conditions) and that this roughly corresponds to the 'rad zone' in the subsurface (see below). Possible Mn concretions or Mn horizons were noted in this

study and in other studies of the Garbutt Formation (Stott, 1982; Leckie and Potocki, 1998). In addition, trace fossils were noted at several levels within the Garbutt Formation, suggesting oxygen levels may have been high enough locally or temporally to allow some organisms to survive. These observations can be explained if these rocks were being deposited close to the anoxic-oxic boundary, which may have fluctuated in response to relative sea level variations and sea water mixing leading to incursions of more oxygenated waters.

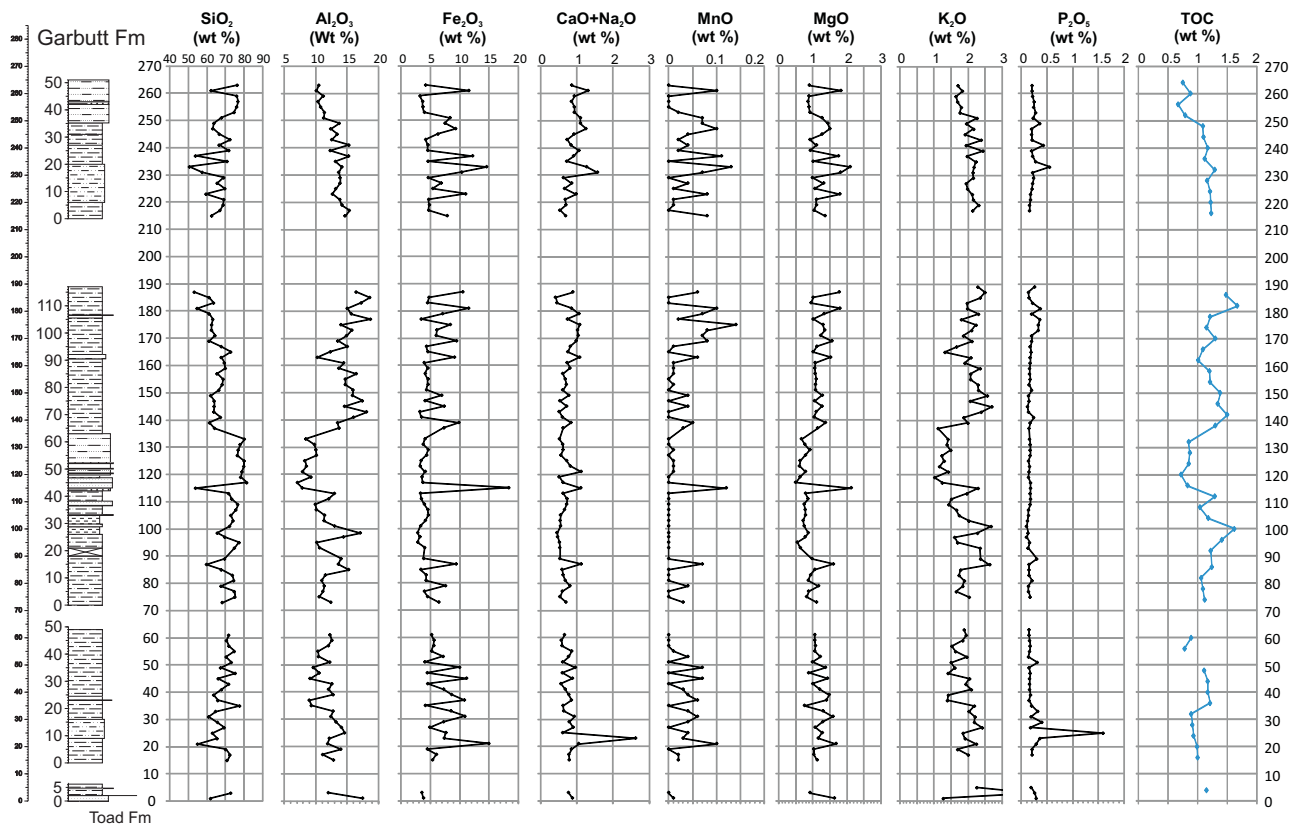


Figure 21. Major oxide geochemical data and total organic carbon contents from the five measured sections of the Garbutt Formation.

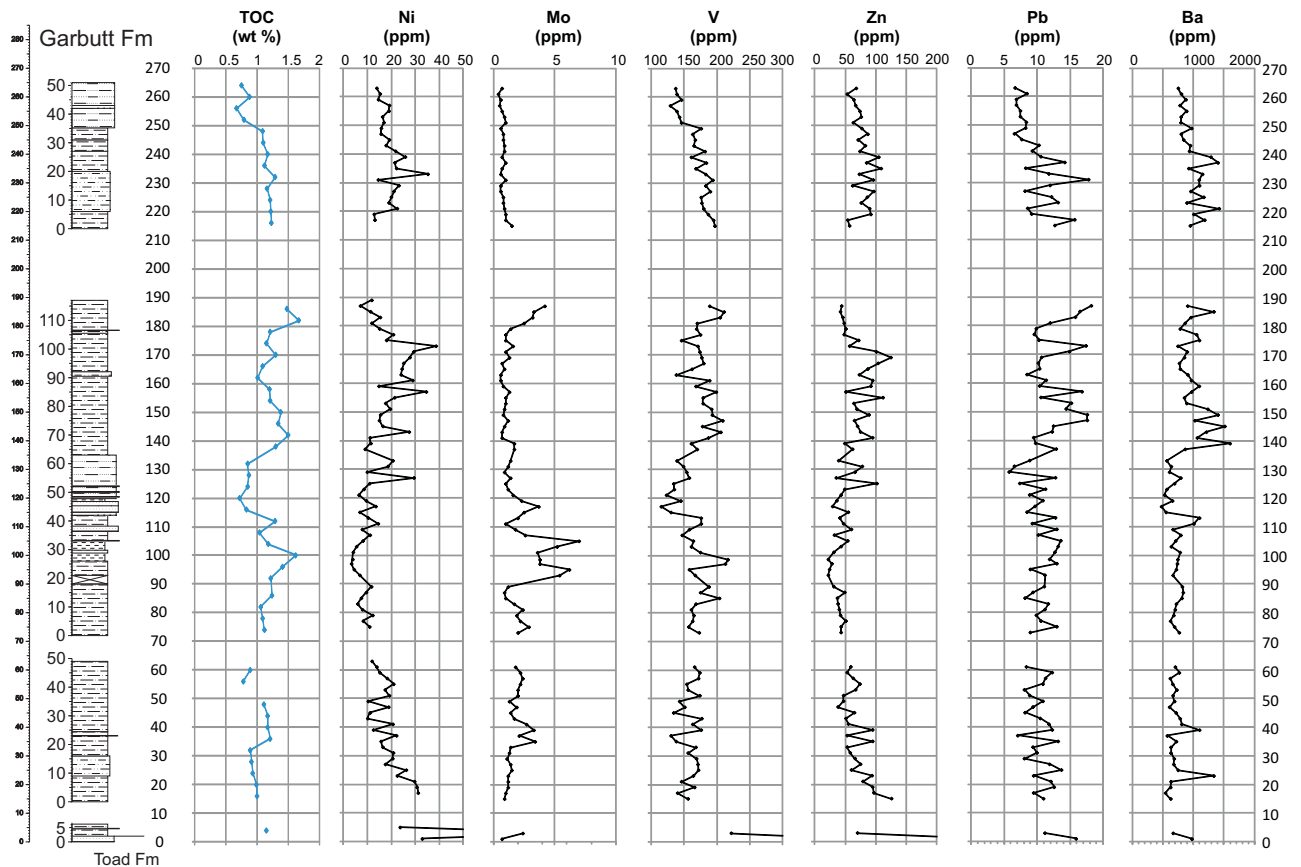


Figure 22. Trace-element data and total organic carbon contents from the five measured sections of the Garbutt Formation.

TABLE 1. SUBDIVISION OF LOW-CALCIC BLACK SHALE BASED ON FE-MN-V CONTENTS.

			Mn ppm	MnO wt. %	Fe ppm	Fe <sub>2</sub> O <sub>3</sub> wt. %	V ppm
Oxygenated waters (Manganese nodules)	Group 1: Oxic Mn>800 ppm, Fe>37,500 ppm, V<320 ppm MnO>0.1%, Fe <sub>2</sub> O <sub>3</sub> >5.36%	Avg.	1,300	0.17	56,000	8.0	130
		Max.	3,600	0.46	87,000	12.4	310
		Min.	830	0.011	38,000	5.4	84
Least Anoxic	Group 2: Mn soluble Mn<750 ppm, Fe<37,500 ppm, V<320 ppm MnO<0.1, Fe <sub>2</sub> O <sub>3</sub> >5.36%	Avg.	310	0.04	52,000	7.4	140
		Max.	730	0.094	100,000	14.3	220
		Min.	46	0.005	39,000	5.6	64
	Group 3: Mn, Fe Soluble Mn<750 ppm, Fe<37,500 ppm, V<320 ppm MnO<0.1%, Fe <sub>2</sub> O <sub>3</sub> <5.36%	Avg.	170	0.022	23,000	3.3	170
		Max.	680	0.088	37,000	5.3	300
		Min.	33	0.004	6,700	0.96	77
Most Anoxic (Maximum preservation of organic matter)	Group 4: V enhanced Mn<750 ppm, Fe<37,500 ppm, V>320 ppm MnO<0.1%, Fe <sub>2</sub> O <sub>3</sub> <5.36%	Avg.	76	0.01	19,000	2.7	1,500
		Max.	260	0.034	36,000	5.1	4,900
		Min.	20	0.003	4,600	0.66	320

(Modified from Quinby-Hunt and Wilde, 1994).

## CORRELATIONS

Correlation of Garbutt Formation rocks examined along Toreva Creek and Scatter River with subsurface sections across the Liard Basin is shown in Figure 23. The constructed gamma-ray trace from this study fits well with the d-98-F well found a few kilometres to the north (Figure 23). Note the change in character of the Garbutt Formation eastward (Figure 23). The most prominent change occurs in the lower third of the formation with the development of the 'rad zone', or radioactive zone, as defined by the anomalous gamma-ray levels at this horizon. The Garbutt Formation also thins and generally becomes finer grained towards the east.

## DISCUSSION

The organic carbon contents and the type of kerogen defined within the Garbutt section of the study area are consistent with those reported by Chalmers and Bustin (2008b). These authors also show organic carbon levels and the type of kerogen within Early Cretaceous sequences changing eastward (i.e., TOC increasing and changing from type III to type II/III and to type I/II kerogen). In the Garbutt Formation, an increase in organic carbon content is indirectly shown by the development of the rad zone in the lower part of the Garbutt Formation, assuming the higher radioactivity is a consequence of an increase in organic carbon.

The eastward increase in TOC levels may be a function of a decrease in sedimentary dilution as one moves away from the western sediment source. Chalmers and Bustin (2008b) suggest that the change from type III to type II/III or type I/II kerogen reflects the proximity of the rock to terrestrial sediment sources (i.e., type III kerogens occurring closer to the sediment supply area). The TOC levels may also increase to the east as a result of better preservation

of organic matter within the deeper, anoxic parts of the basin. Data from this study suggests that Garbutt Formation rocks in the Toreva Creek—Scatter River area were deposited where waters fluctuated between oxic and anoxic conditions. During oxic conditions, organic preservation is likely limited, which may account for lower TOC levels. In addition, organic carbon levels decrease with an increase in thermal maturation as hydrocarbons are produced; this is especially important within type I and II kerogens, where more than half the organic matter is expelled as thermal maturation progresses (Jarvie, 1991). Thermal maturation levels decrease eastward as the sedimentary succession thins, suggesting that residual organic carbon levels should increase if the initial TOC was uniform across the region.

The type (richness) and amount of organic matter within the Garbutt succession appears to decrease towards the Cordilleran front, resulting in a decrease in the amount of adsorbed gas that the sequence can accommodate (see Chalmers and Bustin, 2008a, b). Concurrent with this is an increase in the thickness of the stratigraphic sequence towards the Cordilleran front (i.e., sediment source area), resulting in greater depths of burial and increased formation pressure, which will ultimately increase the amount of gas held within the formations. As a result, the lower adsorbed gas contents due to lower TOC levels will be offset by higher concentrations of pore-space gas.

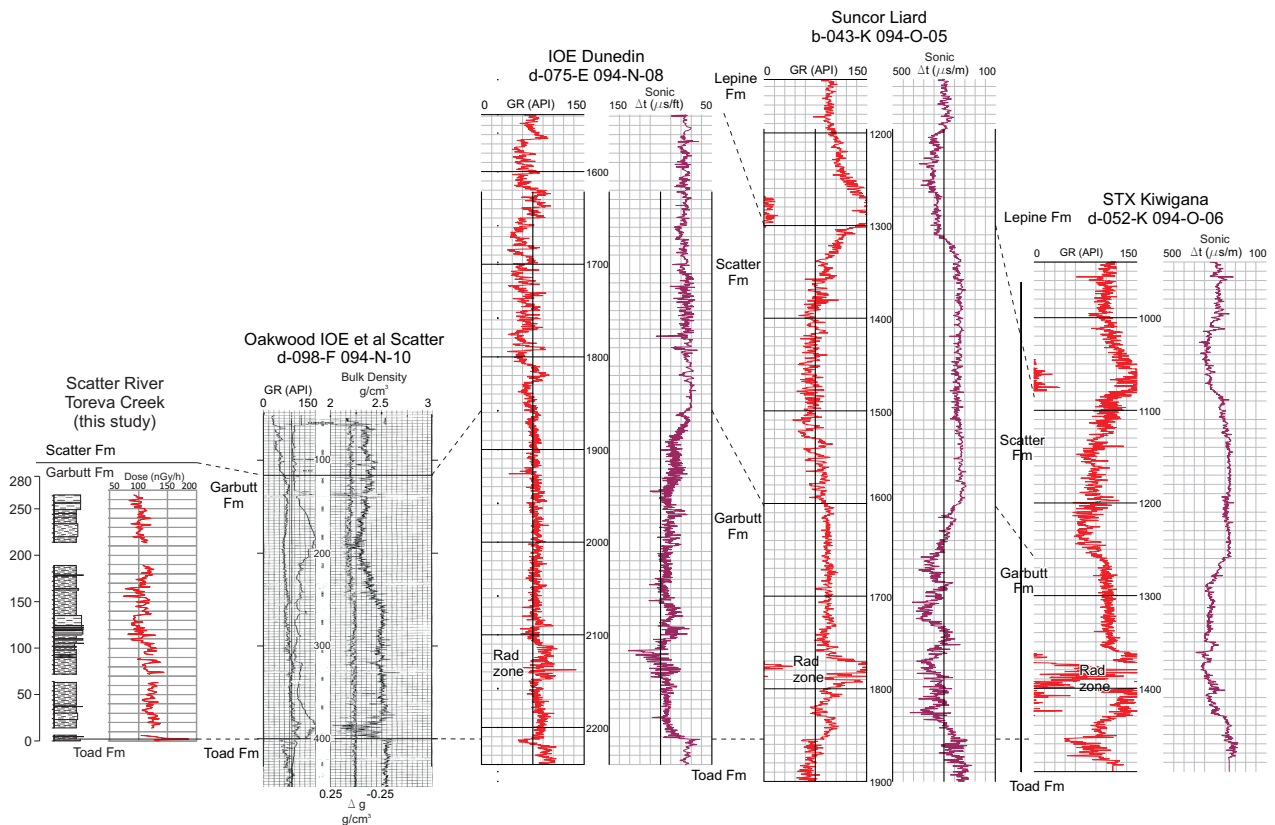


Figure 23. Correlation of the combined five sections of the Garbutt Formation in the study area with several subsurface sections of the unit across the Liard Basin. The location of the wells used in the section can be found in Figure 3.

## CONCLUSIONS

- The Garbutt Formation is approximately 285 m thick in the Toreva—Scatter River area and consists of dark grey to black or dark grey brown shale, siltstone and lesser fine sandstone.
- Sedimentary structures suggest deposition below the storm wave base in a distal shelf, slope-margin or prodelta environment.
- Rock-Eval data show average total organic carbon contents of 1.12 wt.% with peaks between 1.2 and 1.67%. Hydrogen index levels are low and average 60 mg HC/g TOC. Kerogen is type III in nature (terrestrial) and  $T_{max}$  maturation levels suggest the early to mid dry gas generation window.
- The concentration of Mn, Fe, V and other elements suggest that the sediments were deposited near the boundary between anoxic and oxic water conditions.

## ACKNOWLEDGMENTS

The authors thank Lauren Wilson and Lisa Fodor for competent and cheerful assistance in the field. Lisa Fodor is acknowledged for having compiled the scintillometer data. We acknowledge Great Slave Helicopters of Fort Liard for transporting us to our field localities. The senior author thanks Sarah Saad at Geological Survey of Canada laboratories in Calgary for her patience, knowledge in preparation and analysis of Rock-Eval samples.

## REFERENCES

- Adams, C. (2009): Summary of shale gas activity in northeast British Columbia (2008); *BC Ministry of Energy*, Petroleum Geology Open File 2009-1, 17 pages.
- Bordenave, M.L. (1993): Applied Petroleum Geochemistry; *Technip*, 531 pages.
- Chalmers, G.R.L. and Bustin, R.M. (2008a): Lower Cretaceous gas shales in northeastern British Columbia; part I, geological controls on methane sorption capacity; *Bulletin of Canadian Petroleum Geology*, Volume 56, Issue 1, pages 1–21.
- Chalmers, G.R.L. and Bustin, R.M. (2008b): Lower Cretaceous gas shales in northeastern British Columbia; part II, evaluation of regional potential gas resources; *Bulletin of Canadian Petroleum Geology*, Volume 56, Issue 1, pages 22–61.
- Dawson, F.M., Kalkreuth, W.D. and Sweet, A.R. (1992): Stratigraphy and coal resource potential of the Upper Cretaceous to Tertiary strata of northwestern Alberta; *Geological Survey of Canada*, Open File Report 2499, 98 pages.
- Dow, W.G. (1977): Kerogen studies and geological interpretations; *Journal of Geochemical Exploration*, Volume 7, Issue 2, pages 79–99.
- Fallas, K.M. (2001): Preliminary geology, Mount Martin, Yukon Territory—British Columbia—Northwest Territories; *Geological Survey of Canada*, Open File 3402, scale 1:50 000.
- Fallas, K.M. and Evenchick, C.A. (2002): Preliminary geology, Mount Merrill, Yukon Territory—British Columbia; *Geological Survey of Canada*, Open File 4264, scale 1:50 000.
- Fallas, K.M., Pigage, L.C. and MacNaughton, R.B. (2004): Geology, La Biche River southwest (95C/SW), Yukon Territory—British Columbia; *Geological Survey of Canada*, Open File 4664, scale 1:100 000.
- Ferri, F., Golding, M.L., Mortensen, J.K., Zonneveld, J-P. and Orchard, M.J. (2010): Toad Formation (Montney and Doig equivalent) in the northwestern Halfway River map area, British Columbia (NTS 094B/14); in Geoscience Reports 2010, *BC Ministry of Energy, Mines and Petroleum Resources*, pages 21–34.
- Ferri, F., Hickin, A. and Huntley, D. (2011): Besa River Formation, western Liard Basin, British Columbia; geochemistry and regional correlations; in Geoscience Reports 2011, *BC Ministry of Energy*, pages 1–18.
- Ferri, F., Rees, C., Nelson, J. and Legun, A. (1999): Geology and mineral deposits of the northern Kechika Trough between Gataga River and the 60th parallel; *BC Ministry of Forests, Mines and Lands*, Bulletin 107, 122 pages.
- Gabrielse, H. (1963): Geology, Rabbit River, British Columbia; *Geological Survey of Canada*, Preliminary Map 46-1962, scale 1:250 000.
- Gabrielse, H. (1967): Tectonic evolution of the northern Canadian Cordillera; *Canadian Journal of Earth Sciences*, Volume 4, pages 271–298.
- Huntley, D.H. and Hickin, A.S. (2010): Surficial deposits, landforms, glacial history and potential for granular aggregate and frac sand: Maxhamish Lake map sheet (NTS 94O), British Columbia; *Geological Survey of Canada*, Open File 6430, 17 pages.
- Huntley, D. H. and Hickin, A. S. (2011): Geo-Mapping for Energy and Minerals program (GEM-Energy): preliminary surficial geology, geomorphology, resource evaluation and geohazard assessment for the Maxhamish Lake map area (NTS 094O), northeastern British Columbia; in Geoscience Reports 2011, *BC Ministry of Energy*, pages 57–73.
- Huntley, D.H. and Sidwell, C.F. (2010): Application of the GEM surficial geology data model to resource evaluation and geohazard assessment for the Maxhamish Lake map area (NTS 94O), British Columbia; *Geological Survey of Canada*, Open File 6553, 12 pages.
- Huntley, D. H., Hickin, A. S. and Ferri, F. (2011): Provisional surficial geology, glacial history and paleogeographic reconstructions of the Toad River (NTS 094N) and Maxhamish Lake map areas (NTS 094O), British Columbia; in Geoscience Reports 2011, *BC Ministry of Energy*, pages 37–55.
- Jarvie, D.M. (1991): Total organic carbon (TOC) analysis; in Source Migration Processes and Evaluation Techniques, Merrill, R.K., Editor, *American Association of Petroleum Geologists*, Treatise of Petroleum Geology, pages 113–118.
- Jowett, D.M.S. and Schröder-Adams, C.J. (2005): Paleoenvironments and regional stratigraphic framework of the Middle–Upper Albian Lepine Formation in the Liard Basin, Northern Canada; *Bulletin of Canadian Petroleum Geology*, Volume 53, pages 25–50.
- Langford, F.F. and Blanc-Valleron, M.-M. (1990): Interpreting Rock-Eval pyrolysis data using graphs of pyrolyzable hydrocarbons vs. total organic carbon; *American Association of Petroleum Geologists Bulletin*, Volume 74, pages 799–804.
- Leckie, D.A., Kalkreuth, W.D. and Snowdon, L.R. (1988): Source rock potential and thermal maturity of Lower Cretaceous strata; Monkman Pass area, British Columbia; *American Association of Petroleum Geologists Bulletin*, Volume 72, Issue 7, pages 820–838.
- Leckie, D.A. and Potocki, D.J. (1998): Sedimentology and petrography of marine shelf sandstones of the Cretaceous, Scatter and Garbutt formations, Liard Basin, northern Canada; *Bulletin of Canadian Petroleum Geology*, Volume 46, Number 1, pages 30–50.
- Leckie, D.A., Potocki, D.J. and Visser, K. (1991): The Lower Cretaceous Chinkeh Formation: a frontier-type play in the Liard Basin of Western Canada; *American Association of Petroleum Geologists Bulletin*, Volume 75, Number 8, pages 1324–1352.
- Morrow, D.W., Potter, J., Richards, B. and Goodarzi, F. (1993): Paleozoic burial and organic maturation in the Liard Basin region, northern Canada; *Bulletin of Canadian Petroleum Geology*, Volume 41, Issue 1, pages 17–31.
- Mossop, G.D., Wallace-Dudley, K.E., Smith, G.G. and Harrison, J.C., Compilers (2004): Sedimentary basins of Canada; *Geological Survey of Canada*, Open File Map 4673, scale 1:5 000 000.
- Peters, K.E. (1986): Guidelines for evaluating petroleum source rock using programmed pyrolysis; *The American Association of Petroleum Geologists Bulletin*, Volume 70, Number 3, pages 318–329.

- Quinby-Hunt, M.S. and Wilde, P. (1994): Thermodynamic zonation in the black shale facies based on iron-manganese-vanadium content; *Chemical Geology*, Volume 113, Issue 3–4, pages 297–317.
- Richards, B.C., Barclay, J.E., Bryan, D., Hartling, A., Henderson, C.M., Hinds, R.C. and Trollope, F.H. (1994): Carboniferous strata of the Western Canada Sedimentary Basin; in Geological Atlas of the Western Canada Sedimentary Basin; Mossop, G.D. and Shetse, I., Compilers, *Canadian Society of Petroleum Geologists* and *Alberta Research Council*, Special Report 4, URL <[http://www.ags.gov.ab.ca/publications/wcsb\\_atlas/atlas.html](http://www.ags.gov.ab.ca/publications/wcsb_atlas/atlas.html)> [December 2010].
- Stott, D.F. (1982): Late Cretaceous Fort St. John Group and Upper Cretaceous Dunvegan Formation of the Foothills and Plains, Alberta, British Columbia, District of Mackenzie and Yukon Territory; *Geological Survey of Canada*, Bulletin 328, 124 pages.
- Stott, D.F. and Taylor, G.C. (1973): Tuchodi Lakes map area, British Columbia; *Geological Survey of Canada*, Memoir 373, 37 pages.
- Taylor, G.C. and Stott, D.F. (1999): Geology, Toad River, British Columbia; *Geological Survey of Canada*, Map 1955A, scale 1:250 000.
- Teichmuller, M. and Durand, B. (1983): Fluorescence microscopical rank studies on liptinites and vitrinites in peat and coals, and comparison with results of the rock-eval pyrolysis; *International Journal of Coal Geology*, Volume 2, Issue 3, pages 197–230.
- Tissot, B. and Welte, D.N. (1984): Petroleum Formation and Occurrence, 2nd edition; *Springer Verlag*, 699 pages.